

Origin of branched wave structures in optical media and long-tail algebraic intensity distribution

This article has been downloaded from IOPscience. Please scroll down to see the full text article.

2011 EPL 96 44002

(<http://iopscience.iop.org/0295-5075/96/4/44002>)

View [the table of contents for this issue](#), or go to the [journal homepage](#) for more

Download details:

IP Address: 129.219.51.205

The article was downloaded on 29/12/2011 at 21:05

Please note that [terms and conditions apply](#).

Origin of branched wave structures in optical media and long-tail algebraic intensity distribution

XUAN NI^{1(a)}, WEN-XU WANG¹ and YING-CHENG LAI^{1,2}

¹ *School of Electrical, Computer and Energy Engineering, Arizona State University - Tempe, AZ 85287, USA*

² *Department of Physics, Arizona State University - Tempe, AZ 85287, USA*

received 22 July 2011; accepted in final form 26 September 2011

published online 9 November 2011

PACS 42.25.Dd – Wave propagation in random media

PACS 42.25.Bs – Wave propagation, transmission and absorption

PACS 41.20.Jb – Electromagnetic wave propagation; radiowave propagation

Abstract – Experiments have revealed that branched, fractal-like wave patterns can arise in a variety of physical situations ranging from microwave and optical systems to solid-state devices, and that the wave-intensity statistics are non-Gaussian and typically exhibit a long-tail distribution. The origin of branched wave patterns is currently an issue of active debate. We propose and investigate a “minimal” model of optical wave propagation and scattering with two generic ingredients: 1) a finite-size medium for linear wave propagation and 2) random scatterers characterized by a continuous refractive-index profile. We find that branched waves can emerge as a general phenomenon in a wide parameter regime in between the weak-scattering limit and Anderson localization, and the distribution of high intensities follows an algebraic scaling law. The minimal model can provide insights into the physical origin of branched waves in other physical systems as well.

Copyright © EPLA, 2011

Wave propagation through random media occurs in many physical systems, where interesting phenomena such as branched, fractal-like wave patterns or rogue waves can arise. There has been tremendous interest in these complex wave phenomena. For example, in the past decade there were theoretical and experimental studies of rogue waves arising from long-range acoustic wave propagation through ocean’s sound channel [1,2]. Quite recently large-scale experiments on directional ocean waves were conducted to probe the origin of these waves [3]. Similar complex wave patterns arise in many other physical situations such as nonlinear light propagation in doped fibers [4], acoustic turbulence in superfluid helium [5], resonance in nonlinear optical cavities [6], linear light propagation in multi-mode glass fiber [7], and electronic transport in two-dimensional semiconductor electron gas (2DEG) systems [8]. For each of these contexts, there were experimental and theoretical efforts. To illustrate the extent to which branched wave patterns are presently understood, we choose 2DEG systems as an example. In ref. [8], electron flows from a quantum point contact were reported to exhibit a striking, branched or fractal-like

behavior with highly nonuniform amplitude distribution in the physical space. The observed separate, narrow strands of greatly enhanced electron wave intensities were argued to be caused by random background potentials and quantum coherent phase interference among the electron wave functions. Subsequently a theory was proposed [9] to predict the statistical distribution of the intensities of branched electron flows in the presence of weak, correlated Gaussian random potentials. A computational paradigm based on the Green’s function method was also developed [10], providing a systematic way to probe the statistics of branched wave structures in 2DEG systems.

Whether branched, fractal-like wave structures have a generic origin and if yes, it is currently a matter of active debate [11]. A tacit assumption in most previous investigations is nonlinearity in the underlying physical medium. In particular, it was believed that the existence of many uncorrelated, spatially randomly distributed wave elements is key to the occurrence of these exotic wave patterns. These elements can be, *e.g.*, solitons in nonlinear systems. However, quite recently, it was demonstrated experimentally in a microwave system [12] and in a multi-mode optical fiber [7] that branched wave patterns can occur even in the absence of any nonlinearity. In view of

^(a)E-mail: xuan.ni@asu.edu

these conflicting views, it is of fundamental interest to develop a minimal, paradigmatic model that can generate robust branched wave structures. In so doing, a key issue is the statistical properties of branched waves, where analysis of the moments of the intensity distribution dates back to Berry [13] in the context of light-ray caustics. In this regard, a general observation in all situations where branched wave structures emerge is non-Gaussian statistics of wave intensity with an algebraic tail in the probability density function (PDF). A criterion for the validity of any minimal model of branched wave patterns is that it should generate the universally observed, algebraic tail in the wave-intensity distribution.

In this paper, we propose and investigate a minimal model for the emergence and statistical characterization of robust complex branched wave patterns in optical media. Our model contains two basic physical ingredients: 1) a uniform medium of finite size and 2) spatially localized scatterers randomly distributed in the medium, the refractive indices of which deviate from that of the background medium. The second ingredient is required for generating dynamics beyond conventional wave propagation in a linear medium, and we shall demonstrate that our minimal model can generate robust branched, fractal-like wave patterns. Moreover, our model leads naturally to an algebraic, long-tail type of distribution in the wave intensities.

Computationally, we consider a polarized, monochromatic, Gaussian or uniform light beam propagating in a dielectric medium of refractive index n_0 and of size $35 \mu\text{m} \times 70 \mu\text{m}$, which has embedded within itself N random scatterers. The spatial distribution function of the refractive index for the whole system can be written as

$$n(\mathbf{r}) = n_0 + \sum_{i=1}^N \Delta n_i \exp[-|\mathbf{r} - \mathbf{r}_i|^2 / (2\sigma^2)], \quad (1)$$

where each scatterer is characterized by a Gaussian-shaped index distribution of effective radius σ , and \mathbf{r} is a two-dimensional vector in the (x, y) -plane. To simulate the scattering of electromagnetic waves, we use the Finite-Difference Frequency Domain (FDFD) method [14]. Briefly, the method uses Yee's grid, which is a leap-frog discretization scheme for electric and magnetic field components. Instead of solving the Maxwell curl equations directly with time iterations as in the classical FDTD (Finite-Difference Time Domain) scheme, FDFD considers a snapshot of the steady state and uses matrix formulation to solve the whole material system at once [14]. In our simulations, the wavelength is chosen to be $\lambda = 1 \mu\text{m}$. The boundary conditions are properly treated by using Perfect Matched Layers (PMLs) at the boundaries of the material. The scatterers are randomly placed within the material (excluding PMLs), so they do not interact with the PML boundaries. As a result, there are no reflections from the material boundaries.

Figures 1(a)–(c) show a system configuration of 50 random scatterers, the field magnitude from FDFD

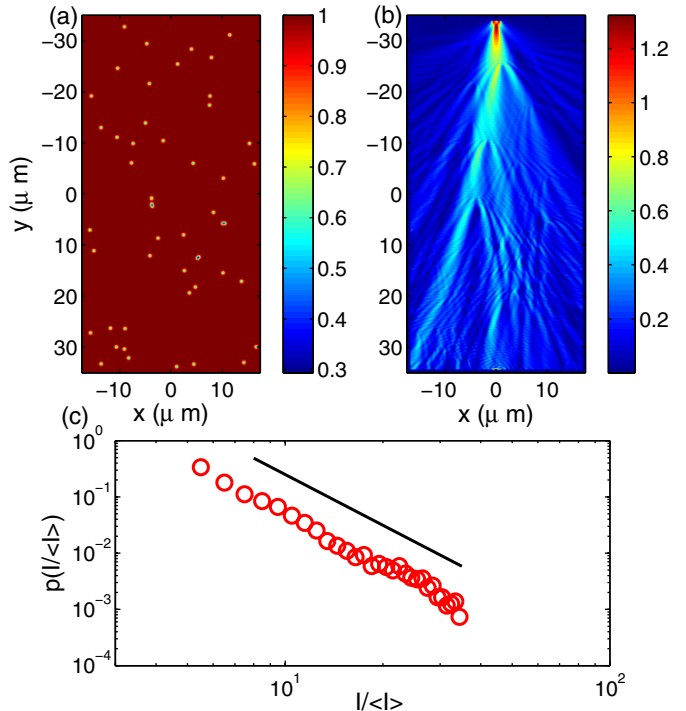


Fig. 1: (Color online) For a rectangular optical medium of size $35 \mu\text{m} \times 70 \mu\text{m}$, (a) spatial distribution of 50 random scatterers, (b) steady-state spatial field-magnitude distribution from FDFD simulations, and (c) scaling behavior of PDF of wave intensity. The PDF is calculated through a histogram statistic of magnitudes of the magnetic components at all lattice sites inside the perfect match layers at the boundaries. The incident wave is uniform of width λ , magnitude $|H_0| = 1$, and sent along the $+y$ direction. The solid line indicates the theoretically predicted scaling law. The simulation parameters are $\lambda = 1 \mu\text{m}$, $n_0 = 1$, $\Delta n = -0.5$, and $\sigma = 0.22 \mu\text{m}$.

simulation, and the intensity distribution on a double-logarithmic scale, respectively. Signatures of fractal-like branched structure are apparent (fig. 1(b)), and the intensity PDF exhibits an algebraic, long-tail behavior. Such behaviors persist when the density of the random scatterers is increased, as shown in fig. 2. While the value of Δn_i is negative for both figs. 1 and 2, branched wave structures have also been observed for positive or mixed values of Δn_i . These simulation results thus suggest the robustness of the branched wave structures in our minimal model. Numerically, we observe that the shape of the refractive-index distribution associated with each random scatterer does not have a significant effect on the emergence and statistical properties of the branched waves. In general, insofar as the sizes of the scatterers are comparable to the wavelength, branched wave patterns can arise.

We now present a theory to explain the emergence of the branched wave structures and the statistical intensity distribution. The general setting is wave propagation in a two-dimensional optical medium with random scatterers.

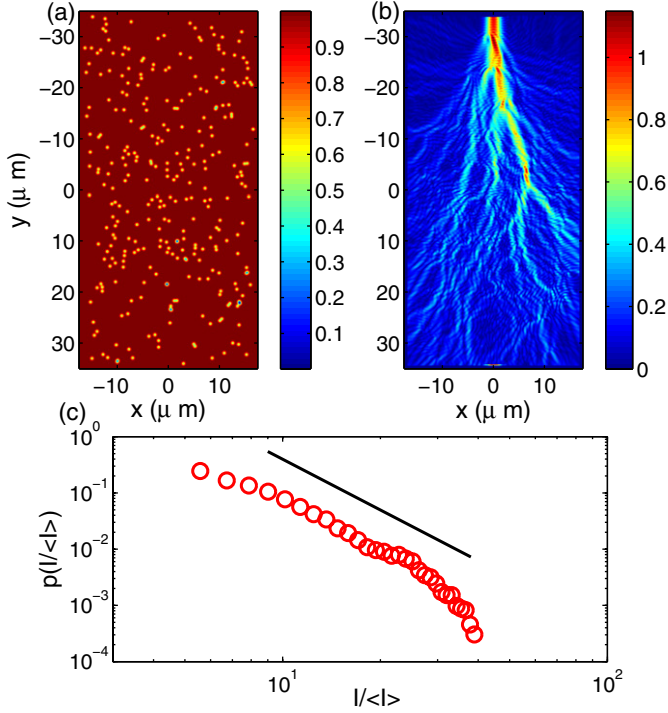


Fig. 2: (Color online) (a) Distribution of 300 random scatterers in the same medium as in fig. 1, (b) wave magnitude from FDFD simulation, and (c) scaling behavior of the intensity distribution. In (c), the deviation from the power-law distribution for high intensity is caused by violation of the sparse-scatterer assumption used in the theory. When the density of scatterers is low, the distribution agrees with theoretical prediction better than that in the high-density case, as shown in fig. 1(c). Other simulation parameters are the same as in fig. 1.

The material is assumed to be isotropic and *linear*, it is neither dispersive nor dissipative, and there is no source (free charge or current). Since all disorders in the refractive index are assumed centro-symmetric in three dimensions, the propagation direction of wave/light with linear polarization is confined within a two-dimensional plane (denoted as the (x,y) -plane). This scheme has been used and justified in ref. [15], where a refractive index profile with large variations was used for studying photonic black holes. For concreteness, we focus on the TE mode, for which the magnetic field strength is given by $\mathbf{H} = H\mathbf{e}_z$. The Maxwell's equations for \mathbf{H} lead to

$$\nabla \times \left(\frac{1}{\varepsilon} \nabla \times \mathbf{H} \right) = k^2 \mu \mathbf{H}, \quad (2)$$

where $k = \omega/c$ is the vacuum wave vector, ε and μ are the relative permittivity and permeability, respectively. The refractive index is $n = \sqrt{\varepsilon\mu}$. The Helmholtz equation for the scalar field H is

$$(\nabla^2 + k^2 n^2) H = (\nabla n/n) \cdot \nabla H. \quad (3)$$

The goal is to calculate the scattering field and its statistical distribution throughout the medium. Our approach

is to first analyze the field from a single scatterer and then extend the result to multiple scatterers. We assume that the random scatterers are far away from each other as compared with their sizes, which can be ensured if they are sparsely distributed in the medium.

Consider a single scatterer located at the origin. Without loss of generality, we set $n_0 = 1$. We decompose the magnetic field H into the incident and scattering parts, *i.e.*, $H = H^i + H^s$. The incident field is a plane wave $H^i = e^{ikx}$, whereas the scattering part is the response of the small scatterer to H^i . Far away from the scatterer, *i.e.*, $r \gg \sigma$, the Helmholtz equation becomes

$$(\nabla^2 + k^2) H^s(\mathbf{r}) = f_1 + f_2 + f_3, \quad (4)$$

where

$$\begin{aligned} f_1(\mathbf{r}) &= -(\nabla^2 + k^2 n^2) H^i, \\ f_2(\mathbf{r}) &= \nabla H^i \cdot \nabla n/n, \\ f_3(\mathbf{r}) &= \nabla H^s \cdot \nabla n/n. \end{aligned}$$

At far field where $H^i \gg H^s$ is satisfied, only f_1 and f_2 contribute to the scattering field in the lowest-order approximation. Also, higher-order corrections due to f_3 can be obtained by Picard iteration and other techniques. The Green's function satisfies

$$(\nabla^2 + k^2) G(\mathbf{r}, \mathbf{r}') = -\delta(\mathbf{r} - \mathbf{r}'). \quad (5)$$

The standard solution to the Green's function in two dimensions is

$$G(\mathbf{r}, \mathbf{r}') = (i/4) H_0^{(1)}(k|\mathbf{r} - \mathbf{r}'|), \quad (6)$$

where $H_0^{(1)} = J_0 + iY_0$ is the Hankel function of the first kind. The scattering field can then be written as

$$H^s(\mathbf{r})_{r \gg \sigma} \approx \sum_{j=1,2} H_j^s(\mathbf{r}), \quad (7)$$

where $H_j^s(\mathbf{r}) = (G * f_j)(\mathbf{r})$ ($j = 1, 2$). The scattering fields due to f_1 and f_2 can be calculated separately. Since disorders are spatially localized and, numerically, we find that the shape of the refractive-index distribution of the scatterer has little effect on the formation of the overall wave pattern, we thus approximate, for distribution from f_1 , the refractive index as

$$n^2(\mathbf{r}) \approx \begin{cases} (1 + \Delta n)^2 - \Delta n(1 + \Delta n) \left[\frac{r}{\alpha\sigma} \right]^2, & r \leq r_b, \\ 1, & r > r_b, \end{cases} \quad (8)$$

where

$$r_b = \alpha\sigma \sqrt{\frac{\Delta n + 2}{\Delta n + 1}} \quad (9)$$

is the boundary of the scatterer, and α is the parameter that controls the width of variation in n^2 . Similar approximation can be applied to calculating the contribution from f_2 . We have

$$\nabla n/n \approx \begin{cases} -\frac{\Delta n}{\Delta n + 1} \frac{[1 - \beta r^2 / (2\sigma^2)] \mathbf{r}}{\sigma^2}, & r \leq r'_b, \\ 0, & r > r'_b, \end{cases} \quad (10)$$

where $r'_b = \sigma\sqrt{2/\beta}$ and β serves the same role as α . These approximated forms of the refractive index-related function profiles allow us to evaluate *analytically* the scattering field at far field by integrating the convolutions, which requires the asymptotic form of the Hankel function at far field:

$$H_0^{(1)}(x \gg 1/4) \sim (\pi x/2)^{-1/2} \exp[i(x - \pi/4)]. \quad (11)$$

A lengthy algebra to evaluate the integral contained in $H^s(\mathbf{r})_{r \gg \sigma}$ leads to the following expression of the scattering field:

$$H^s(r, \phi)_{r \gg r_b, r'_b} \approx \frac{e^{ikr}}{r^{1/2}} \Phi(\phi) + \frac{e^{ikr}}{r^{3/2}} \Psi(\phi), \quad (12)$$

where

$$\begin{aligned} \Phi(\phi) &= a_{11}\Phi_1(\phi) + a_{21}\Phi_2(\phi), \\ \Psi(\phi) &= a_{12}\Psi_1(\phi) + a_{22}\Psi_2(\phi), \end{aligned}$$

and a_{ij} 's are constants that depend on the wave vector k , the parameters Δn , r_b , r'_b and σ^2 . To the lowest order $r^{-1/2}$, the scattering field is

$$H^s \approx r^{-1/2} \exp(ikr) \Phi(\phi), \quad (13)$$

where the functions $\Phi_1(\phi)$ and $\Phi_2(\phi)$ are given by

$$\begin{aligned} \Phi_1(\phi) &= J_2(kr_b \sqrt{2 - 2 \cos \phi}) / (2 - 2 \cos \phi), \\ \Phi_2(\phi) &= J_3(kr'_b \sqrt{2 - 2 \cos \phi}) / \sqrt{2 - 2 \cos \phi}, \end{aligned} \quad (14)$$

and Ψ_1 and Ψ_2 are also generalized hypergeometric functions. While eq. (12) is derived under the assumption $n_0 = 1$, the cases where n_0 is not unity can be treated by using the simple substitutions $k \rightarrow kn_0$ and $\Delta n \rightarrow \Delta n/n_0$.

Note that in eq. (14), the size of scatterer is reflected in the angular part of the scattering field. This means that the scatterer size will affect the number of branches in the field. We have examined that small changes in the size of scatterers will not affect the PDF to any notable extent. However, very large scatterers will cause the branched structure to disappear. The extreme case of large scatterers corresponds actually to the short-wavelength limit, where geometric optics can be used to describe the behavior of light rays. In this case, intensity statistics become meaningless.

The scattering field structure calculated directly from eq. (12) is shown in fig. 3. We see that, in the forward direction, the strength of the scattering field damps with the radius and the field is composed of a series of magnified flows radiating in all directions, which capture the typical behavior of the scattering field obtained from direct FDFD simulations. Note that in fig. 3, both the $r^{-1/2}$ and $r^{-3/2}$ terms have been taken into account, but the $r^{-3/2}$ term is at least two orders of magnitude weaker than the $r^{-1/2}$ term, providing further justification for using only the first term in eq. (12).

Our expression for the scattering field of a single scatterer provides a qualitative explanation as to why a highly

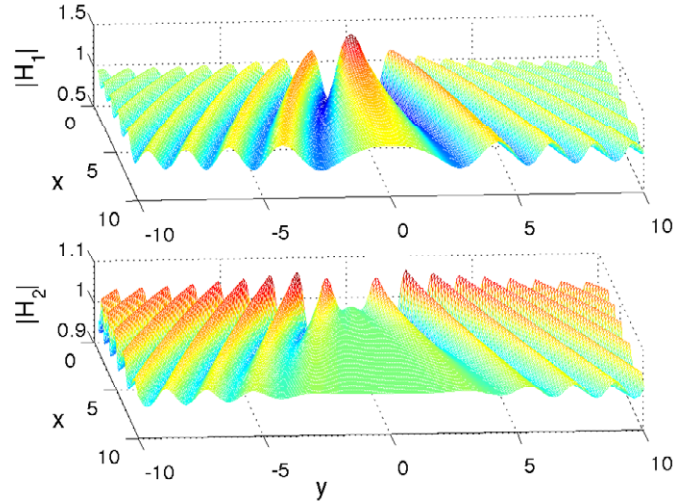


Fig. 3: (Color online) Forward scattering field from a single scatterer. The wave (of wavelength $\lambda = 1 \mu\text{m}$) is incident in the forward (+ x) direction on a scatterer located at the origin. The parameters characterizing the refractive-index function of the scatterer are $\sigma = 0.22 \mu\text{m}$ and $\Delta n = -0.5$. The two plots $|H_1|$ and $|H_2|$ including the $r^{-1/2}$ and $r^{-3/2}$ terms are from f_1 and f_2 , respectively.

nonuniform field structure can arise. In particular, the analytic result explains, instead of a uniform spread of the scattering field in all directions, it tends to form a branched structure with hot spots. Multiple scatterers make the branched structure finer. In particular, each scattering event gives rise to a few dominant branches that spread out into the far field. Some of the remaining scatterers are within the large branches while most other scatterers are located outside any large branched structure. The scatterers in the latter group are essentially not affected by the scattering field. Second-stage scattering will also induce some large branches, which can possibly “meet” with the branches from the first-stage scattering and generate constructive interference. Significantly finer and highly localized structure of the field can result from such interference. The probabilities of destructive and constructive interferences are approximately the same. However, since the higher-level scattering fields are necessarily weaker than the ancestor wave branches, the already generated intense branches cannot be eliminated, especially for the branches near the center direction of the propagation. This provides a plausible explanation as to why in most cases of branched waves the strongest branch either is along the center direction or tilts slightly to one side. The former is due to equal probabilities that random scatterers appear on both sides of the main propagation direction, and the latter is caused by the asymmetric distribution of the refractive index of the scatterer on both sides. This branch-accumulation process is extremely sensitive to the spatial distribution of the refractive index, leading to the emergence of hierarchical, fractal-like wave patterns.

We now calculate the scattering field intensity from multiple scatterers. Let the subscript 0 denote infinity where the incident wave is originated, and assume that the incident wave beam is first scattered by only one scatterer, labeled by 1. Treating the field point j as another scatterer, we obtain the total field from all possible scattering paths

$$q_{0,1,j} + \sum_i q_{0,1,i} q_{1,i,j} + \sum_{i,\ell} q_{0,1,i} q_{1,i,\ell} q_{\ell,i,j} + \dots, \quad (15)$$

where the cumulative factor $q_{i,j,\ell}$ can be derived by applying eq. (12) to calculating the resulting field from three consecutive points along the scattering path. We obtain

$$q_{i,j,\ell} = \frac{e^{ik|\mathbf{r}_j - \mathbf{r}_i|}}{\sqrt{|\mathbf{r}_j - \mathbf{r}_i|}} \cdot \Phi[\cos^{-1}(\mathbf{e}_{ij} \cdot \mathbf{e}_{j\ell})], \quad (16)$$

where \mathbf{e}_{ij} is the unit vector associated with $\mathbf{r}_j - \mathbf{r}_i$. Since the scatterers are randomly distributed, the summation over the same scattering level will not cause any order-of-magnitude change in the scattering field, due to the fact that complex variables of similar magnitude but of random phases will cancel each other, generating a number located close to the origin of the complex plane. In order to obtain the statistical properties of high-intensity spots that are located close to the scatterers, we need to make approximations on each $q_{i,j,\ell}$ term. Specifically, we write

$$q_{i,j,\ell} \approx q = \rho^{-1/2} \exp(ik\rho)\Phi(\varphi), \quad (17)$$

where ρ is the distance between each pair of scatterers and φ is the angle determined by the relative positions of the three consecutive scatterers. Using this model, the sum of the first m terms in the series becomes $S_m = q + q^2 + q^3 + \dots + q^m$. Let $q = ae^{i\theta}$, where $a \geq 0$. We get the sum of the geometric series

$$S_\infty = \frac{ae^{i\theta}}{1 - ae^{i\theta}}. \quad (18)$$

Similar to geometric series of real numbers, $a \in [0, 1)$ is the condition that guarantees the convergence of the sum. In our case, this condition is satisfied because we assume weakly correlated scatterers so that $a \rightarrow 0$. The total intensity of the scattering field is then

$$I(\rho, \varphi) = |S_\infty|^2 = \left| \frac{ae^{i\theta}}{1 - ae^{i\theta}} \right|^2. \quad (19)$$

To the lowest order, we obtain $I = |\Phi(\varphi)|^2/\rho$, which is similar to the formula for the single-scatterer case. This is reasonable because, under the assumption of weakly correlated scatterers, contributions from higher-level scattering processes are small for most points in the space.

The probability distribution of the intensity of the scattering field can be obtained if the distributions of the

position parameters ρ and φ are available. To be concrete, denote $f_{\rho,\varphi}(\rho, \varphi)$ as the joint PDF of random variables ρ and φ . The expression $I = I(\rho, \varphi)$ alone is not sufficient to derive the PDF of the intensity. What is needed is an auxiliary function $J = J(\rho, \varphi)$. We have

$$f_I(I) = \int f_{I,J}(I, J) dJ = \int \frac{f_{\rho,\varphi}(\rho(I, J), \varphi(I, J))}{\left| \det \left(\frac{\partial(I, J)}{\partial(\rho, \varphi)} \right) \right|} dJ, \quad (20)$$

where $\partial(I, J)/\partial(\rho, \varphi)$ is the Jacobian matrix associated with the corresponding transform. The joint PDF of the variables in the polar coordinate is proportional to the unit area of the two-dimensional plane, $f_{\rho,\varphi} \sim \rho$, and a convenient choice for $J(\rho, \varphi)$ is $J = \varphi$. We then obtain the following algebraic scaling law of the PDF of the intensity of the scattering field:

$$f_I(I) \propto I^{-\gamma}, \quad (21)$$

where the scaling exponent is $\gamma = 3$ for our minimal model to the lowest order.

To verify the algebraic scaling law, we have carried out extensive FDFD computations for different realizations of random scatterers of different densities, as exemplified by figs. 1(c) and 2(c). From these results (and many others cases as well), we observe branched wave patterns and the associated algebraic scaling law for the intensity distribution, as predicted by our theory. Especially, when the random scatterers are weakly correlated, the algebraic scaling behavior is robust, implying the existence of ‘‘hot’’ branches with extremely high local intensities. As the density of the random scatterers is decreased, this hallmark of branched waves tends to be somewhat weakened because, when the scatterers are further apart, the intensity of the wave scattered from one scatterer may already have weakened significantly before reaching the next scatterer, making it less probable for fields from different levels of scattering to interfere constructively.

In summary, we proposed a minimal model to probe into the origin of branched, fractal-like wave patterns. We have established, through computations and an analytic theory, that robust branched wave structures can emerge in a wide range of system parameters with algebraic (power-law) tails in the distribution of the intensity, regardless of the difference in the physical properties of the random scatterers. Our analysis suggests that branched wave patterns in physical systems can be caused by the following two mechanisms: 1) break-up of wave by a single scatterer, and 2) constructive interference of ‘‘broken waves’’ by multiple scatterers randomly located in the space. Note that these two mechanisms are fairly ‘‘elementary’’ in wave physics, and we believe that they explain why branched structures arise as a universal phenomenon in all kinds of wave systems. Although our computations and analysis are for optical waves, the physical insights should be applicable to many other wave systems in various areas of science and engineering as well.

We thank Dr V. KOVANIS from AFRL for stimulating discussions. This work was supported by AFOSR under Grant No. FA9550-09-1-0026.

REFERENCES

- [1] WHITE B. S., *J. Fluid Mech.*, **355** (1998) 113; ONORATO M., OSBORNE A. R. and SERIO M., *Phys. Rev. Lett.*, **96** (2006) 014503; AKHMEDIEV N., SOTO-CRESPO J. M. and ANKIEWICZ A., *Phys. Lett. A*, **373** (2009) 2137; ELIASSON B. and SHUKLA P. K., *Phys. Rev. Lett.*, **105** (2010) 014501; HAMMANI K., KIBLER B., FINOT C. and PICOZZI A., *Phys. Lett. A*, **374** (2010) 3585.
- [2] WOLFSON M. A. and TOMSOVIC S., *J. Acoust. Soc. Am.*, **109** (2001) 2693; BERON-VERA F. J., BROWN M. G., COLOSI J. A., TOMSOVIC S., VIROVLYANSKY A. L., WOLFSON M. A. and ZASLAVSKY G. M., *J. Acoust. Soc. Am.*, **114** (2003) 1226; BROWN M. G., COLOSI J. A., TOMSOVIC S., VIROVLYANSKY A. L., WOLFSON M. A. and ZASLAVSKY G. M., *J. Acoust. Soc. Am.*, **113** (2003) 2533.
- [3] ONORATO M., WASEDA T., TOFFOLI A., CAVALERI L., GRAMSTAD O., JANSSEN P. A. E. M., KINOSHITA T., MONBALIU J., MORI N., OSBORNE A. R., SERIO M., STANSBERG C. T., TAMURA H. and TRULSEN K., *Phys. Rev. Lett.*, **102** (2009) 114502.
- [4] SOLLI D. R., ROPERS P., KOONATH C. and JALALI B., *Nature (London)*, **450** (2007) 1054; DUDLEY J. M., GENTY G. and EGGLETON B., *Opt. Express*, **16** (2008) 3644.
- [5] GANSHIN A. N., EFIMOV V. B., KOLMAKOV G. V., MEZHOV-DEGLIN L. P. and MCCLINTOCK P. V. E., *Phys. Rev. Lett.*, **101** (2008) 065303.
- [6] MONTINA A., BORTOLOZZO U., RESIDORI S. and ARECCHI F. T., *Phys. Rev. Lett.*, **103** (2009) 173901.
- [7] ARECCHI F. T., BORTOLOZZO U., MONTINA A. and RESIDORI S., *Phys. Rev. Lett.*, **106** (2011) 153901.
- [8] TOPINKA M. A., LEROY B. J., WESTERVELT R. M., SHAW S. E. J., FLEISCHMANN R., HELLER E. J., MARANOWSKI K. D. and GOSSARD A. C., *Nature*, **410** (2001) 183.
- [9] KAPLAN L., *Phys. Rev. Lett.*, **89** (2002) 184103.
- [10] METALIDIS G. and BRUNO P., *Phys. Rev. B*, **72** (2005) 235304.
- [11] AKHMEDIEV N. and PELINOVSKY E., *Eur. Phys. J. ST*, **185** (2010) 1 and articles therein.
- [12] HÖHMANN R., KUHL U., STÖCKMANN H.-J., KAPLAN L. and HELLER E. J., *Phys. Rev. Lett.*, **104** (2010) 093901.
- [13] BERRY M. V., *J. Phys. A: Math. Gen.*, **10** (1977) 2061.
- [14] See, for example, WU S.-D. and GLYTSIS E. N., *J. Opt. Soc. Am. A*, **19** (2002) 2018; YU C.-P. and CHANG H.-C., *Opt. Express*, **12** (2004) 1397.
- [15] GENOV D. A., ZHANG S. and ZHANG X., *Nat. Phys.*, **5** (2009) 687.